Wedelolactone promotes the chondrogenic differentiation of mesenchymal stem cells by suppressing EZH2 in both methyltransferase activity-dependent and -independent manner

wei Qin (qinwei2017210@163.com)
Guangzhou University of Chinese Medicine https://orcid.org/0000-0002-8249-5777
Lin Yang
Shenzhen Traditional Chinese Medicine Hospital
Xiaotong Chen
Third Affiliated Hospital of Sun Yat-Sen University
Shanyu Ye
Guangzhou University of Traditional Chinese Medicine: Guangzhou University of Chinese Medicine
Aijun Liu
Guangzhou University of Traditional Chinese Medicine: Guangzhou University of Chinese Medicine
Dongfeng Chen
Guangzhou University of Traditional Chinese Medicine: Guangzhou University of Chinese Medicine
Kunhua Hu
Third Affiliated Hospital of Sun Yat-Sen University

Research Article

Keywords: Wedelolactone, chondrogenic differentiation, EZH2, FOXO1, miR-1271-5p

Posted Date: February 4th, 2022

DOI: https://doi.org/10.21203/rs.3.rs-1310903/v1

Abstract

Background: Osteoarthritis (OA) is a degenerative disease that leads to the progressive destruction of articular cartilage. Current clinical therapeutic strategies are moderately effective at relieving pain, but often cannot induce chondrocyte differentiation and achieve cartilage regeneration. Wedelolactone, an active chemical ingredient derived from *Eclipta alba*, has been reported to facilitate osteoblastogenesis but inhibits adipogenesis in MSCs. However, the effects of wedelolactone on chondrogenic differentiation of MSCs remain largely unknown.

Methods: Human-induced pluripotent stem cell (iPSC)-derived MSCs and rat bone marrow MSCs were treated with wedelolactone. Then, real-time reverse transcription-polymerase chain reaction (RT-PCR), immunohistochemical staining, and immunofluorescence staining were used to evaluate the effects of wedelolactone on chondrogenic differentiation of MSCs. To explore the potential mechanism of the effects of wedelolactone on chondrogenic differentiation of MSCs, we performed RNA-seq, miRNA-seq, isobaric tags for relative and absolute quantitation (iTRAQ) analysis, and ChIP-qPCR.

Results: We demonstrated that wedelolactone had a beneficial effect on the chondrogenic differentiation of human-induced pluripotent stem cell (iPSC)-derived mesenchymal stem cells (MSCs) and rat bone marrow MSCs. Notably, the forkhead box O (FOXO) signaling pathway was upregulated by wedelolactone during chondrogenic differentiation. The FOXO1 inhibitor attenuated the effect of wedelolactone on chondrocyte differentiation. Mechanistically, wedelolactone reduced the enhancer of zeste homolog 2 (EZH2)-mediated histone 3 lysine 27 trimethylation (H3K27me3) on the promoter region of FOXO1 to increase its transcription. Additionally, wedelolactone repressed microRNA (miR)-1271-5p expression in an EZH2-mediated H3K27me3 independent manner. Further, miR-1271-5p post-transcriptionally suppressed FOXO1 expression dependent on the binding of miR-1271-5p to the FOXO1 3'-UTR.

Conclusion: These results indicate that wedelolactone suppresses EZH2 to facilitate the chondrogenic differentiation of MSCs by activating the FOXO1 signaling pathway, suggesting that wedelolactone might improve cartilage regeneration in diseases characterized by inflammatory tissue destruction, such as OA.

Introduction

Injury and aging-related disorders of the cartilage often result in the development of degenerative joint diseases, such as osteoarthritis (OA)[1]. OA is characterized by the progressive destruction of articular cartilage, suggesting a key role of chondrocytes in the pathogenesis of OA. Although chondrocytes have low mitotic activity, they are responsible for the synthesis and turnover of the articular cartilage matrix. With the onset of OA, chondrocytes undergo multiple changes in their proliferation, viability, and secretory profile[2]. Current drugs for OA mostly aim to relieve the pain and inflammation. Regenerative strategies for the use of drugs to stimulate chondrogenesis in endogenous stem cells and increase the cartilage matrix of chondrocytes are still lacking.

Recent studies have shown that there is a population of cartilage stem/progenitor cells, similar to populations of mesenchymal stem cells (MSCs) found in bone marrow, which may be involved in cartilage repair and maintenance of chondrocyte homeostasis. These cartilage stem/progenitor cells have been observed in human, equine, and bovine articular cartilage and have been characterized based on the expression levels of stem cell-related surface markers. Phenotypic analyses have shown that cartilage stem/progenitor cells express various MSC-related surface markers, including cluster of differentiation (CD)-29 (integrin β-1), CD44, CD105, etc[3]. Therefore, a better understanding of the mechanisms involved in the differentiation of MSCs into chondrocytes may enable the screening of therapeutic drugs that promote chondrogenic differentiation of cartilage stem/progenitor cells and abnormal cartilage repair in OA.

Wedelolactone is suggested to be the active component of *Ecliptae herba*. It possesses anti-inflammatory activities, including the inhibition of IkappaB kinase, thereby reducing the phosphorylation of both IkappaB and nuclear factor (NF)-kappa B[4]. Our previous study showed that wedelolactone promoted Ser/Thr phosphorylation of NLR family pyrin domain-containing 3, which is dependent on protein kinase A signaling to block inflammasome activation[5]. Moreover, recent studies, including ours, have shown the effects of wedelolactone on MSCs. Wedelolactone has been reported to inhibit the adipogenic differentiation of human adipose tissue-derived MSCs[6]. In addition, Liu et al. demonstrated that wedelolactone enhances osteoblastogenesis, but inhibits osteoclastogenesis of MSCs[7–9]. Another study showed that wedelolactone stimulates odontoblast differentiation[10]. However, the effects of wedelolactone on chondrogenic differentiation of MSCs remain largely unknown.

The pharmacological activity of wedelolactone was attributed to the inhibition of the IkappaB kinase, caspase-11, and/or androgen receptors. Emerging evidence indicates that wedelolactone can act independently of IkappaB kinase, caspase-11, or androgen receptors[11–13]. For example, the anti-tumor effects of wedelolactone may be due to the inhibition of DNA topoisomerase IIα[14]. Wedelolactone was also found to have potent G protein-coupled receptor-35 agonist activity[15]. Importantly, recent studies have demonstrated that wedelolactone can target the enhancer of zeste homolog 2 (EZH2)-embryonic ectoderm development (EED) complex to promote histone H3K27 demethylation, indicating that wedelolactone is a promising epigenetic agent for cancer treatment[16]. Thus, the major cellular targets and the exact mechanisms of wedelolactone are context-dependent and remain to be identified.

In this study, we used human induced pluripotent stem cell (iPSC)-derived MSCs and rat bone marrow MSCs to investigate the effect of wedelolactone on chondrogenic differentiation. Intriguingly, compared to the control media, MSCs exposed to wedelolactone-containing media showed a significant increase in chondrocyte differentiation. We also showed that forkhead box O 1 (FOXO1) was stimulated by wedelolactone during chondrogenic differentiation. The mechanism by which wedelolactone induces the FOXO1 pathway in chondrocyte differentiation was subsequently investigated.

Materials And Methods

Cell culture.

Human iPSC (hiPSC) line was obtained from the American Type Culture Collection (ATCC-BYS0113). The hiPSCs were maintained on Matrigel (Corning)-coated dishes in PeproGrow-hESC (PeproTech) medium containing 2 μM Y-27632. The medium was changed every day. All cells were cultured at 37 °C in a humidified atmosphere of 5% CO2 and 95% air.

The hiPSCs were then induced to form EBs. Briefly, iPSCs were digested and resuspended in EB differentiation medium (iPSC culture medium without β-FGF) and then transferred to ultra-low adhesion 6-well plate (Corning). The differentiation medium was changed every 2 days. After 10 days, the EBs were transferred into culture plates with 0.1% gelatin-coated (Corning) and cultured for another 3 days. Then cells were digested and digested solution was filtered through 100 μm nylon mesh. Cells were resuspended in the MSCs growth medium, which consisted of DMEM (Gibco) supplemented with 10% fetal bovine serum (FBS; Gibco), MEM Non-Essential Amino Acids (Gibco), 2ng/ml FGF (PeproTech), 20ng/ml EGF (PeproTech).

Collection and culture of bone marrow mesenchymal stem cells (BMSCs)

The tibia and femur of SD rats were isolated under sterile conditions. Next, the tibia and femur were put into cooled PBS and washed away the attached blood. The bone marrow cavity was washed by DMEM medium containing 10% FBS repeatedly. The cells of bone marrow cavity were flushed into a sterile culture dish and cultured in an incubator containing 5% CO2 at 37 ℃. After 24h, the nonadherent cells were gently washed off with PBS, and the MSCs growth medium was changed every three days.

Flow Cytometric analysis

The hiPSC derived MSCs were washed with PBS, harvested by 0.25% trypsin/EDTA, and resuspended in 100 μl staining media (2% FBS and 2% HEPES in PBS) and stained with mouse anti-human CD29 (BD), mouse anti-human CD44 (BD), mouse anti-human CD34 (BD), mouse anti-human CD105 (BD), and mouse anti-human CD45 (BD) for 30 min at 4°C. Isotype-matched antibody (IgG2b-FITC) was used to determine nonspecific fluorescence. Samples were run on CytoFLEX (BECKMAN) instrument. A minimum of 20,000 cells was assayed for each analysis.

Chondrogenic differentiation of MSCs

For chondrogenic differentiation of MSCs[17, 18], 5×10^5 hiPSC derived MSCs or rat bone marrow MSCs cells were centrifuged at 500 g for 10 min to form a small pellet in a 15 ml centrifuge tube. The cell pellets were cultured for 21 days in the chondrogenic differentiation medium consisting of DMEM (Gibco)

supplemented with 10 % FBS, 1:100 ITS-G (ThemoFisher), 100 nM dexamethasone, 10 ng/mL recombinant TGF-β3 (PeproTech), 40 μg/ml L-proline (Sigma-Aldrich). The medium was changed every 3 days.

Rat cartilage defect model

We established a rat cartilage defect model as previously described[19]. The 8-week-old SD rats were anesthetized through intraperitoneal injection of ketamine. The skin around the knee was disinfected, and the right knee of rats was exposed by surgery. Next, a defect (diameter 1.5 mm and 1.5 mm in depth) was created in the center of the groove. The rats were divided into two groups, the experimental group was implanted into hydrogel mixed with rat bone marrow MSCs which were treated with or without wedelolactone. After 6 weeks, all rats were sacrificed, and joint tissues were collected for further analyzed.

Alcian blue staining and toluidine blue staining of chondrocytes

MSCs were seeded in a 6-well plate, then cells were induced in chondrogenic differentiation medium for 3 days. Then the medium was removed and cells were washed with PBS for 3 times. The cells were stained with toluidine blue staining solution or alcian blue staining solution for 30 minutes. Next, the cells were washed with PBS for 5 minutes. Then the stained cells were observed under a microscope.

Histology staining of chondrogenic pellets

Chondrogenic pellets were collected after 21 days of chondrogenic differentiation. Then the pellets were fixed in 4% buffered formaldehyde for 6 hours. Next, these pellets were dehydrated in different concentrations of alcohol. After clarified in the pellet in xylene three times, the pellets were infiltrated with paraffin for 1 h in a 65 °C oven. Then, these pellets were sliced at 7 μm for histology staining. The slides were deparaffinized by moving them through 200 mL of 100%, 95%, 80%, and 75% EtOH sequentially for 4 min each. The slides were incubated in 3% H_2O_2 for 15 min for endogenous peroxidase blocking. Then, the slides were blocked with goat serum solution at room temperature for 10-15 minutes, Incubated with 100 μL of primary antibodies (anti-COL2A1 or anti-ACAN) at 4 °C for overnight. After slides were washed with PBS 3 times, they were incubated with an appropriate amount of biotin-labeled goat anti-mouse/rabbit IgG polymer at room temperature for 15 minutes. The slides were washed with PBS for 3 times, then incubated with an appropriate amount of horseradish enzyme-labeled streptomyces ovalbumin working solution for 10 to 15 minutes. Next slides were washed with PBS 3 times and incubated with DAB solution for 5 to 8 minutes. Last, these stained slides were observed under a microscope.

MSCs were cultured with chondrogenic differentiation medium for 3 days in confocal dishes. The cells were fixed with 4% paraformaldehyde (dissolved in PBS, pH 7.4) for 10 minutes at room temperature. Next, the cells were incubated with PBS (containing 0.1-0.25% Triton X-100) for 10 minutes. Then, the cells were incubated with goat serum at room temperature for 30 minutes to block the nonspecific binding of antibodies. After that, the cells were incubated with 100 μL of primary antibodies (anti-COL2A1, anti-ACAN, and anti-SOX9) at 4 °C for overnight. The next day, the cells were washed 3 times with PBS and then incubated with second antibodies for 1h at room temperature. DAPI was used to stain nuclei. The stained cells were observed under a confocal microscope.

Chromatin immunoprecipitation quantitative PCR

The ChIP assay was performed as previously described[20]. Briefly, the cells were seeded in a 10 cm dish, and then the cells were cross-linked with 1% paraformaldehyde for 10 min. The cells were incubated with glycine to terminate the cross-linking. The cells were lysed on ice, and were centrifugated at 12000×g. The nuclei of the cells were resuspended in the lysis solution. The chromatin DNA of the cells was sonicated. 30 μl protein A-agarose beads were added to the mixture. Then the mixture was incubated with H3K27me3 antibody, EZH2 antibody, or control immunoglobulin G (IgG) for 2 h at 4 °C. Subsequently, the antibody/protein/DNA complex was eluted from the beads. The remaining proteins and RNAs were degraded with protease K and RNase A. The DNA was extracted with phenol-chloroform and purified with a PCR purification kit.

iTRAQ (isobaric Tags for Relative and Absolute Quantitation) and TMT (Tandem Mass Tags)

Chondrogenic pellets were lysed by adding an appropriate amount of lysate solution and then heated at 95 ℃ for 10min. The mixture was centrifuged at 12000×g for 10 minutes, the supernatant was transferred to a new 1.5 ml tube. DTT (dithiothreitol) was added to the supernatant. The protein solution was transferred to a 10 K ultrafiltration tube for centrifugation. Then, the collected solution was discarded, and replaced with a new one. Trypsin was added into the ultrafiltration tube. The proteins were enzymatically hydrolyzed at 37 ℃ for 16 h. The enzymatically hydrolyzed polypeptide was concentrated and then labeled by iTRAQ regent. The iTRAQ-labeled samples were analyzed using Liquid Chromatography with Tandem Mass Spectrometry (Thermo Fisher Easy-nlC 1000 Liquid Chromatograph and Thermo Fisher Q Exactive).

Statistical analysis

All statistical analyses were processed using SPSS 10.0 software. Data are presented as mean ± SD. All the data are presented of three independent experiments. Comparisons between three groups were

performed using one-way analysis of variance (ANOVA). Comparisons between two groups were performed using a two-sided Student's t-test. For all tests, Statistical significance was set at $p < 0.05$.

Results

Wedelolactone promotes the differentiation of human iPSC-derived MSCs to chondrocytes in vitro

Using a modified stepwise protocol, we derived human MSCs from an iPSC line established from a healthy donor (Fig. 1a; Fig. S1a). A homogeneous culture of hiPSC-derived MSCs had a fibroblastic spindle-shaped morphology that resembled bone marrow MSCs and expressed CD29, CD44, and CD105, but not CD45 or CD34 (Fig. S1b). To evaluate the effects of wedelolactone on chondrogenesis, we cultured hiPSC-derived MSCs with and without wedelolactone during chondrogenic differentiation using a previously reported protocol (Fig. 1a). Chondrogenic pellets were formulated after 21 d of chondrogenic differentiation (Fig. 1b). Next, we observed an upregulation in the gene expression levels of SRY-box transcription factor 9 (*SOX9*), collagen type II alpha-1 (*COL2A1*), and aggrecan (*ACAN*) in hiPSC-derived MSC chondrogenic pellets after 21 d of chondrogenicdifferentiation (Fig. 1c). Meanwhile, the gene expression levels of these cartilage markers increased further after wedelolactone treatment (Fig. 1c). Immunohistochemical results also showed a significant upregulation of COL2A1 and ACAN after wedelolactone treatment (Fig. 1d). We also observed increased protein expression levels of COL2A1, ACAN, and SOX9 after wedelolactone treatment under 2D culture conditions (Fig. 1e; Fig. S1c, d). These data indicate that wedelolactone can significantly promote the chondrogenic differentiation of human iPSC-derived MSCs.

Wedelolactone promotes the chondrogenic differentiation of rat bone marrow MSCs

To further confirm the role of wedelolactone in promoting chondrogenic differentiation, we used another differentiation system, as previously reported[21]. Rat bone marrow MSCs were induced to differentiate into chondrocytes using induction media under 3D culture conditions, with and without wedelolactone (Fig. 2a). Chondrogenic pellets were formed after 21 d of chondrogenic differentiation (Fig. 2b). Next, we observed a significant increase in the gene expression levels of chondrogenic markers (*COL2A1*, *ACAN*, and *SOX9*) after wedelolactone treatment (Fig. 2c). Wedelolactone also upregulated the protein levels of these chondrogenic markers during chondrogenic differentiation of rat bone marrow MSCs (Fig. 2d, e).

To confirm the beneficial effect of wedelolactone in promoting cartilage regeneration in *vivo*, rat bone marrow MSCs were induced with or without wedelolactone in the chondrogenic differentiation medium for three days. Then, the cells were mixed with the hydrogel and injected into the cartilage defect rat model (Fig. 2f). Through the morphological staining results of saffron solid green, we found that wedelolactone-treated cells showed a better repair effect on cartilage defects (Fig. 2g). In summary, these

results indicate that wedelolactone can promote the differentiation of rat bone marrow MSCs into chondrocytes *in vitro* and cartilage repair *in vivo*.

Wedelolactone promotes the chondrogenic differentiation of MSCs by activating the FOXO pathway

To explore the underlying mechanism of wedelolactone in the regulation of chondrogenic differentiation of MSCs, we performed RNA-seq and iTRAQ-based quantitative proteomic analysis on human iPSC-derived MSCs treated with dimethyl sulfoxide (DMSO) or wedelolactone during chondrogenic differentiation. The iTRAQ analysis data showed that 1,108 proteins were upregulated and 185 proteins were downregulated upon wedelolactone treatment (Fig. 3a). Meanwhile, RNA-seq analysis revealed that 812 genes were upregulated under wedelolactone treatment (Fig. S2a). The Kyoto Encyclopedia of Genes and Genomes analysis demonstrated that the differentially expressed genes or proteins were enriched in the FOXO signaling pathway (Fig. 3b; Fig. S2b). Interestingly, the FOXO signaling pathway factors were upregulated in the wedelolactone-treated samples (Fig. 3c). Previous studies have reported that wedelolactone enhances osteoblastogenesis by regulating the Wnt and extracellular signal-regulated kinase (ERK) pathways. However, the gene set enrichment analysis results revealed that wedelolactone had no effect on the WNT, ERK, or NF-κB signaling pathways during chondrogenic differentiation (Fig. S2c).

Recent research has shown that FOXOs are key factors in stem cell maintenance and differentiation. We observed that wedelolactone increased the gene expression level of *FOXO1* during chondrogenic differentiation in *vitro* (Fig. 3d). Moreover, in the cartilage defect model, wedelolactone-treated rat bone marrow MSCs expressed more FOXO1 in *vivo* compared to control MSCs (Fig. 3e). To investigate the effects of FOXO1 on chondrogenic differentiation, we silenced *FOXO1* in human iPSC-derived MSCs during chondrogenic differentiation. Alcian blue and toluidine blue staining results showed that glycosaminoglycan formation was decreased upon *FOXO1* knockdown (Fig. 3f). Real-time reverse transcription-polymerase chain reaction (RT-PCR) results showed that the gene expression levels of chondrogenic markers (*COL2A1, ACAN*, and *SOX9*) were significantly increased in *FOXO1* knockdown cells (Fig. 3g). Additionally, AS1842856, a specific FOXO1 inhibitor, significantly decreased glycosaminoglycan formation in iPSC-derived MSCs compared with that in the control group (Fig. S2d). Moreover, the gene expression levels of chondrogenic markers were significantly decreased after AS1842856 treatment (Fig. S2e). These findings proved that FOXO1 is an important regulatory factor in chondrogenic differentiation.

The promoting effect of wedelolactone on chondrogenic differentiation could be weakened by FOXO1 inhibitor

To further confirm that FOXO1 is a key regulatory factor in the process of wedelolactone regulation of chondrogenic differentiation, we tested the effects of FOXO1 inhibitor on wedelolactone-treated cells. Alcian blue staining and toluidine blue staining results showed that the FOXO1 inhibitor significantly decreased glycosaminoglycan formation induced by wedelolactone during chondrogenic differentiation. Furthermore, wedelolactone did not alleviate the inhibitory effect of the FOXO1 inhibitor during chondrogenic differentiation (Fig. 4a). Real-time RT-PCR results showed that the gene expression levels of chondrogenic markers (COL2A1, ACAN, and SOX9) were significantly increased after wedelolactone treatment but completely abolished under wedelolactone and FOXO1 inhibitor combination treatment (Fig. 4b). These results indicate that FOXO1 is a key regulatory factor in the process of wedelolactone-mediated regulation of chondrogenic differentiation.

Wedelolactone decreases EZH2-dependent trimethylation of histone 3 lysine 27 (H3K27me3) on the promoter region of FOXO1

We then explored the potential mechanisms by which wedelolactone upregulated the expression of FOXO1 during chondrogenic differentiation. Immunoblot analysis showed that wedelolactone decreased the protein level of H3K27me3 and increased FOXO1 protein expression levels (Fig. S3a). Moreover, the chromatin immunoprecipitation-quantitative polymerase chain reaction (ChIP-qPCR) results showed that wedelolactone decreased the modification of H3K27me3 on the promoter of *FOXO1* in human iPSC-derived MSCs and 293T cells (Fig. 5a). As a histone methyltransferase, EZH2 inhibits gene transcription through the trimethylation of H3K27me3. Next, we used GSK126, an effective and highly selective EZH2 methyltransferase inhibitor to intervene in H3K27me3 during chondrogenic differentiation. As expected, GSK126 increased the expression of FOXO1 at both the mRNA and protein levels (Fig. 5b, c).

To verify whether FOXO1 is a repression target of EZH2 during chondrogenic differentiation, we used ChIP-qPCR assay and proved that EZH2 could bind to the *FOXO1* promoter in human iPSC-derived MSCs and 293T cells (Fig. 5d). Moreover, we observed that *EZH2* silencing in human iPSC-derived MSCs caused a significant upregulation of FOXO1 expression at both the mRNA and protein levels during chondrogenic differentiation (Fig. 5f, g). In contrast, overexpression of EZH2 in human iPSC-derived MSCs led to downregulation of FOXO1 expression (Fig. 5e). Wedelolactone had no effect on FOXO1 gene expression levels in *EZH2* KD human iPSC-derived MSCs (Fig. 5h), suggesting that wedelolactone increases FOXO1 expression by targeting EZH2 in an H3K27me3 dependent manner.

miR-1271-5P interferes with the expression of FOXO1 during chondrogenic differentiation

As an important form of post-transcriptional regulation, miRNAs play a biological role by regulating their downstream gene translation processes. To investigate the potential post-transcriptional regulatory

mechanisms of FOXO1, we performed miRNA-seq on human iPSC-derived MSCs treated with or without wedelolactone during chondrogenic differentiation (Fig. 6a). Eighteen miRNAs were upregulated and 111 were downregulated upon chondrogenic differentiation (Fig. 6b). Venn diagram analysis showed that two miRNAs (miR-12136 and miR3648-5P) were upregulated after chondrogenic differentiation and further upregulated after wedelolactone treatment (Fig. 6c; Fig. S4a). Four miRNAs (miR-1271-5P, miR-22-3P, miR-1296-5P, and miR-361-5P) were downregulated after chondrogenic differentiation and further downregulated after wedelolactone treatment (Fig. 6d; Fig. S4b). These six miRNAs might play an important role in the effects of wedelolactone on chondrogenic differentiation.

We predicted the target genes of these six miRNAs using the TargetScan and miRDB databases. We observed that *FOXO1* is a potential target gene of miR-1271-5P (Fig. 6e). To test whether miR-1271-5P directly targets FOXO1, we constructed luciferase reporters that had either a wild-type 3'-untranslated region (UTR) (FOXO1-3'-UTR-wt) or a 3'-UTR containing mutant (FOXO1-3'-UTR-mut) sequences of the miR-1271-5P binding site. We found that overexpression of miR-1271-5P strongly inhibited the luciferase reporter activity of the WT FOXO1 3'-UTR, but not that of the mutated 3'-UTR (Fig. 6f). Further experiments confirmed that miR-1271-5P overexpression obviously decreased FOXO1 protein expression (Fig. 6g). These results indicate that FOXO1 is a target gene of miR-1271-5P. To explore the mechanism of EZH2 on the expression of miR-1271-5P, we silenced EZH2 in human iPSC-derived MSCs during chondrogenic differentiation. We found that the expression of miR-1271-5P was remarkably decreased after *EZH2* KD (Fig. 6h). However, the expression of miR-1271-5P did not differ after GSK126 treatment (Fig. 6i). Therefore, EZH2 regulates the expression of miR-1271-5P in an H3K27me3-independent manner.

Discussion

Previous studies have reported that wedelolactone has antihemorrhagic and antiproteolytic activity, and it facilitates osteoblastogenesis but inhibits adipogenesis in MSCs[6, 22]. However, the effects of wedelolactone on the differentiation of MSCs into chondrocytes have not been studied. In this study, we demonstrated that wedelolactone promotes chondrocyte differentiation in both human iPSC-derived MSCs and rat bone marrow MSCs. The expression of chondrocyte marker genes, *COL2A1* and *SOX9*, was significantly up-regulated upon wedelolactone treatment. Intriguingly, we reveals a novel role for wedelolactone in facilitating chondrocyte differentiation by increasing the FOXO1 signaling pathway by suppressing EZH2 in both methyltransferase activity-dependent and -independent manner (Fig. 7), suggesting that wedelolactone might promote cartilage repair and increase the cartilage matrix in OA.

Wedelolactone is known to exert regulatory effects on inflammation by suppressing the iKK/NF-kB signaling pathway[4]. However, the mechanism by which wedelolactone affects stem cell differentiation is not well understood. Previous reports have demonstrated that wedelolactone enhances osteoblastogenesis by regulating WNT and ERK pathways[9]. In this study, our proteomic data indicated that wedelolactone did not affect WNT, ERK, or NF-κB signaling pathways in chondrocyte differentiation. This discrepancy might be due to the cell type- and context-dependent effects of wedelolactone on stem cell differentiation. The master transcription factor in chondrogenesis is SOX9, which controls the

expression of key chondrocyte-specific genes. We showed that wedelolactone increased SOX9 expression during chondrogenic differentiation of MSCs. Moreover, EZH2 catalyzes the deposition of methyl groups on H3K27 for gene silencing. It has been reported that the overexpression of EZH2 suppressed the expression of SOX9 in rat endplate chondrocytes (EPCs)[23]. Therefore, wedelolactone might suppresses H3K27me3 at the SOX9 promoter during chondrogenic differentiation of MSCs.

Our data also suggest that wedelolactone potently increased FOXO1 dependent signaling pathways. FOXO proteins are transcription factors that play important roles in stem cell differentiation[24, 25]. The function of FOXO3A in chondrogenic differentiation of MSCs has been well-studied[26, 27]. A recent study and our RNA-seq data showed that FOXO1 expression increased along with chondrogenic differentiation. In addition, Kurakazu et al. showed that FOXO1 inhibition led to cell cycle arrest and chondrogenic differentiation suppression via TGFβ1 signaling[28]. Indeed, we found that inhibition of FOXO1 activity by AS1842856, a specific FOXO1 inhibitor, significantly attenuated the beneficial effects of wedelolactone on the chondrogenesis of MSCs. A previous study reported that ectopic overexpression of EZH2 decreased FOXO1 expression in human oral squamous cell carcinoma cells[29]. We hypothesized that wedelolactone might regulate the expression of FOXO1 during chondrogenic differentiation via EZH2 modulation. Hence, we investigated the mechanism of regulation of FOXO1 expression upon wedelolactone treatment in chondrogenesis. First, we confirmed that gene expression of FOXO1 increased by EZH2 inhibitor treatment during chondrogenic differentiation. Furthermore, we showed that EZH2 binds to the promoter of FOXO1. This is consistent with the observation that EZH2 inhibition reduced the H3K27me3 on promoter of FOXO1.

To date, the functions and underlying mechanisms of EZH2 in chondrogenesis have not been completely elucidated. During stem cell differentiation or embryonic development, EZH2 mediates the silencing of a diverse group of developmental genes and reshapes the epigenetic landscape in an H3K27me3 dependent way[30, 31]. However, Camilleri et al. showed that EZH2 activity is dispensable for normal chondrocyte maturation. They found that although EZH2 deficiency resulted in a global reduction of H3K27me3 in chondrocytes, conditional knockout mice show normal cartilage development[32]. Another group showed that EZH2 expression was significantly higher in the chondrocytes of OA patients than in normal humans. Intra-articular injection of EZH2 inhibitor delayed OA development in mice model[33]. These findings imply that EZH2 may have physiological and pathological roles in normal or OA chondrocytes by modulating different downstream signaling pathways. Our study does not rule out the possibility of EZH2 in regulating other targets in chondrogenic differentiation, but does highlight the importance of FOXO1 as EZH2 targets in chondrocytes.

Finally, we demonstrated that the noncanonical role of EZH2 as a transcriptional activator for miR-1271-5p expression coexists with its conventional catalytic role as a gene repressor of FOXO1 in chondrogenic differentiation. Interestingly, emerging evidence suggests noncanonical roles of EZH2 in various cell types. For example, Li et al. showed that EZH2 binds to the promoter of methyltransferase-like 3 to activate its expression in an H3K27me3 independent manner in glioblastoma. Moreover, EZH2 can directly methylate Jarid2 to regulate its transcriptional activity during cell differentiation. In our study, the

enzymatic EZH2 inhibitor, GSK126, was unable to suppress miR-1271-5p expression. Instead, depletion of EZH2 by specific short hairpin RNAs decreased miR-1271-5p expression. Our results suggest that wedelolactone can block the dual roles of EZH2. Therefore, small-molecule inhibitors should be developed as effective therapeutic agents for the treatment of OA in future studies.

Conclusion

In summary, we demonstrated that wedelolactone reduced the enhancer EZH2 mediated H3K27me3 on the promoter region of FOXO1 to increase its transcription. Additionally, wedelolactone repressed miR-1271-5p expression in an EZH2-mediated H3K27me3 independent manner. Further, miR-1271-5p post-transcriptionally suppressed FOXO1 expression dependent on the binding of miR-1271-5p to the FOXO1 3'-UTR. At last, the expression of FOXO1 was upregulated during chondrogenic differentiation after Wedelolactone intervention.

Abbreviations

OA: Osteoarthritis; iPSC: Human induced pluripotent stem cell; MSCs: Mesenchymal stem cells; iMSCs: Human induced pluripotent stem cell derived mesenchymal stem cells; BMSCs: Bone marrow-derived mesenchymal stem cell; FOXO1: Forkhead box O 1; EZH2: Zeste homolog 2; H3K27me3: Histone 3 lysine 27 trimethylation; iTRAQ: Isobaric tags for relative and absolute quantitation; TMT: Tandem mass tags; SOX9: SRY-box transcription factor 9; COL2A1: Collagen type II alpha-1; ACAN: aggrecan; DMSO: Dimethyl sulfoxide; KEGG: Kyoto encyclopedia of genes and genomes; ERK: Extracellular signal-regulated kinase; RT-PCR: Real-time reverse transcription-polymerase chain reaction; ChIP-Qpcr: Chromatin immunoprecipitation-quantitative polymerase chain reaction;

Declarations

Acknowledgements

We would like to thank Dr. Wei Zhao for valuable suggestions. We also thank all of the students who participated in this study.

Authors’ contributions

W. Q. performed the human iPSC-derived MSC differentiation experiments and wrote the manuscript. L. Y., X. C., and S. Y. performed rat MSC differentiation assays and the animal experiments. A. L. interpreted the data and revised the manuscript. D. C. and K. H. designed the experiments, interpreted the data, wrote the manuscript, and provided supervision.

Funding

This work was supported by Guangdong Innovative and Entrepreneurial Research Team Program (2016ZT06S029), the Natural Science Foundation of Guangdong Province (2017A030312009) and the China Postdoctoral Science Foundation (2021M700961).

Availability of data and materials

The data that support the findings of this study are available from the corresponding author upon reasonable request.

Ethics approval and consent to participate

Ethical approval for use of experimental rats was granted by the University's Ethics Review Board.

Consent for publication

Not applicable

Competing interests

The authors declare that they have no competing interests.

Author details

[1]Research Center for Integrative Medicine, School of Basic Medical Sciences, Guangzhou University of Chinese Medicine, Guangzhou 510006, China. [2]Shenzhen Hospital of Integrated Traditional Chinese and Western Medicine, Shenzhen 518101, China. [3]Guangdong Key Laboratory of Liver Disease Research, the Third Affiliated Hospital of Sun Yat-sen University, Guangzhou 510630, China

References

1. Martel-Pelletier J, Barr AJ, Cicuttini FM, Conaghan PG, Cooper C, Goldring MB, et al. Osteoarthritis Nat Reviews Disease Primers. 2016;2(1). doi:10.1038/nrdp.2016.72.
2. Xie J, Wang Y, Lu L, Liu L, Yu X, Pei FJArr. Cellular senescence in knee osteoarthritis: molecular mechanisms and therapeutic implications. 2021;70:101413. doi: 10.1016/j.arr.2021.101413. PubMed PMID: 34298194.
3. Jiang Y, Tuan RJNrR. Origin and function of cartilage stem/progenitor cells. osteoarthritis. 2015;11(4):206–12. doi:10.1038/nrrheum.2014.200. PubMed PMID: 25536487.

4. Zhu M, Wang L, Yang D, Li C, Pang S, Li X, et al. Wedelolactone alleviates doxorubicin-induced inflammation and oxidative stress damage of podocytes by IκK/IκB/NF-κB pathway. 2019;117:109088. doi: 10.1016/j.biopha.2019.109088. PubMed PMID: 31202173.
5. Pan H, Lin Y, Dou J, Fu Z, Yao Y, Ye S, et al. Wedelolactone facilitates Ser/Thr phosphorylation of NLRP3 dependent on PKA signalling to block inflammasome activation and pyroptosis. 2020;53(9):e12868. doi: 10.1111/cpr.12868. PubMed PMID: 32656909.
6. Lim S, Jang H, Park E, Kim J, Kim J, Kim E, et al. Wedelolactone inhibits adipogenesis through the ERK pathway in human adipose tissue-derived mesenchymal stem cells. 2012;113(11):3436–45. doi: 10.1002/jcb.24220. PubMed PMID: 22678810.
7. Deng X, Liang L, Zhu D, Zheng L, Yu J, Meng X, et al. Wedelolactone inhibits osteoclastogenesis but enhances osteoblastogenesis through altering different semaphorins production. 2018;60:41–9. doi: 10.1016/j.intimp.2018.04.037. PubMed PMID: 29702282.
8. Liu Y, Han X, Bo J, Ma HJFip. Wedelolactone Enhances Osteoblastogenesis but Inhibits Osteoclastogenesis through Sema3A/NRP1/PlexinA1 Pathway. 2016;7:375. doi: 10.3389/fphar.2016.00375. PubMed PMID: 27803667.
9. Liu Y, Hong Z, Zhan L, Chu H, Zhang X, Li GJSr. Wedelolactone enhances osteoblastogenesis by regulating Wnt/β-catenin signaling pathway but suppresses osteoclastogenesis by NF-κB/c-fos/NFATc1 pathway. 2016;6:32260. doi: 10.1038/srep32260. PubMed PMID: 27558652.
10. Wang C, Song Y, Gu Z, Lian M, Huang D, Lu X, et al. Wedelolactone Enhances Odontoblast Differentiation by Promoting Wnt/β-Catenin Signaling Pathway and Suppressing NF-κB. Signaling Pathway. 2018;20(4):236–44. doi:10.1089/cell.2018.0004. PubMed PMID: 30089027.
11. Idris A, Libouban H, Nyangoga H, Landao-Bassonga E, Chappard D, Ralston SJMct. Pharmacologic inhibitors of IkappaB kinase suppress growth and migration of mammary carcinosarcoma cells in vitro and prevent osteolytic bone metastasis in vivo. 2009;8(8):2339–47. doi: 10.1158/1535-7163.Mct-09-0133. PubMed PMID: 19671767.
12. Xu S, Liu X, Liu X, Shi Y, Jin X, Zhang N, et al. Wedelolactone ameliorates Pseudomonas aeruginosa-induced inflammation and corneal injury by suppressing caspase-4/5/11/GSDMD-mediated non-canonical pyroptosis. 2021:108750. doi: 10.1016/j.exer.2021.108750. PubMed PMID: 34481822.
13. Nehybova T, Smarda J, Daniel L, Brezovsky J. Benes PJTJosb, biology m. Wedelolactone induces growth of breast cancer cells by stimulation of estrogen receptor signalling. 2015;152:76–83. doi: 10.1016/j.jsbmb.2015.04.019. PubMed PMID: 25934092.
14. Benes P, Knopfova L, Trcka F, Nemajerova A, Pinheiro D, Soucek K, et al. Inhibition of topoisomerase IIα: novel function of wedelolactone. 2011;303(1):29–38. doi: 10.1016/j.canlet.2011.01.002. PubMed PMID: 21315506.
15. Deng H, Fang Y. Anti-inflammatory gallic Acid and wedelolactone are G protein-coupled receptor-35 agonists. Pharmacology. 2012;89(3-4):211–9. Epub 2012/04/11. doi: 10.1159/000337184. PubMed PMID: 22488351.

16. Romanchikova N, Trapencieris, PJAr. Wedelolactone Targets EZH2-mediated Histone H3K27 Methylation in Mantle Cell Lymphoma. 2019;39(8):4179–84. doi: 10.21873/anticanres.13577. PubMed PMID: 31366503.
17. Nam Y, Rim YA, Ju JH. Chondrogenic Pellet Formation from Cord Blood-derived Induced Pluripotent Stem Cells. J Vis Exp. 2017;(124). Epub 2017/06/28. doi: 10.3791/55988. PubMed PMID: 28654049; PubMed Central PMCID: PMCPMC5608467.
18. Li Y, Hai Y, Chen J, Liu T. Differentiating Chondrocytes from Peripheral Blood-derived Human Induced Pluripotent Stem Cells. J Vis Exp. 2017;(125). Epub 2017/07/27. doi: 10.3791/55722. PubMed PMID: 28745632; PubMed Central PMCID: PMCPMC5612544.
19. Bi R, Yin Q, Mei J, Chen K, Luo X, Fan Y, et al. Identification of human temporomandibular joint fibrocartilage stem cells with distinct chondrogenic capacity. 2020;28(6):842–52. doi: 10.1016/j.joca.2020.02.835. PubMed PMID: 32147536.
20. Li F, Chen S, Yu J, Gao Z, Sun Z, Yi Y, et al. Interplay of m(6) A and histone modifications contributes to temozolomide resistance in glioblastoma. Clin Transl Med. 2021;11(9):e553. doi:10.1002/ctm2.553. PubMed PMID: 34586728; PubMed Central PMCID: PMCPMC8441140. Epub 2021/09/30.
21. Xu M, Stattin EL, Shaw G, Heinegard D, Sullivan G, Wilmut I, et al. Chondrocytes Derived From Mesenchymal Stromal Cells and Induced Pluripotent Cells of Patients With Familial Osteochondritis Dissecans Exhibit an Endoplasmic Reticulum Stress Response and Defective Matrix Assembly. Stem Cells Transl Med. 2016;5(9):1171–81. doi:10.5966/sctm.2015-0384. PubMed PMID: 27388238; PubMed Central PMCID: PMCPMC4996445. Epub 2016/07/09.
22. Zhu D, Deng X, Han X, Sun X, Pan T, Zheng L, et al. Wedelolactone Enhances Osteoblastogenesis through ERK- and JNK-mediated BMP2 Expression and Smad/1/5/8 Phosphorylation. 2018;23(3). doi: 10.3390/molecules23030561. PubMed PMID: 29498687.
23. Jiang C, Guo Q, Jin Y, Xu J, Sun Z, Zhu D, et al. Inhibition of EZH2 ameliorates cartilage endplate degeneration and attenuates the progression of intervertebral disc degeneration via demethylation of Sox-9. 2019;48:619–29. doi: 10.1016/j.ebiom.2019.10.006. PubMed PMID: 31631036.
24. Ludikhuize M, Meerlo M, Gallego M, Xanthakis D, Burgaya Julià M, Nguyen N, et al. Mitochondria Define Intestinal Stem Cell Differentiation Downstream of a FOXO/Notch Axis. 2020;32(5):889-900.e7. doi: 10.1016/j.cmet.2020.10.005. PubMed PMID: 33147486.
25. Kim D, Hwang I, Muller F. Paik JJCd, differentiation. Functional regulation of FoxO1 in neural stem cell differentiation. 2015;22(12):2034–45. doi: 10.1038/cdd.2015.123. PubMed PMID: 26470727.
26. Guérit D, Brondello J, Chuchana P, Philipot D, Toupet K, Bony C, et al. FOXO3A regulation by miRNA-29a Controls chondrogenic differentiation of mesenchymal stem cells and cartilage formation. 2014;23(11):1195–205. doi: 10.1089/scd.2013.0463. PubMed PMID: 24467486.
27. Djouad F, Bony C, Canovas F, Fromigué O, Rème T, Jorgensen C, et al. Transcriptomic analysis identifies Foxo3A as a novel transcription factor regulating mesenchymal stem cell chrondrogenic differentiation. 2009;11(3):407–16. doi: 10.1089/clo.2009.0013. PubMed PMID: 19751111.

28. Kurakazu I, Akasaki Y, Hayashida M, Tsushima H, Goto N, Sueishi T, et al. FOXO1 transcription factor regulates chondrogenic differentiation through transforming growth factor β1 signaling. 2019;294(46):17555–69. doi: 10.1074/jbc.RA119.009409. PubMed PMID: 31601652.
29. Zheng M, Cao M, Luo X, Li L, Wang K, Wang S, et al. EZH2 promotes invasion and tumour glycolysis by regulating STAT3 and FoxO1 signalling in human OSCC cells. 2019;23(10):6942–54. doi: 10.1111/jcmm.14579. PubMed PMID: 31368152.
30. Yu Y, Deng P, Yu B, Szymanski J, Aghaloo T, Hong C, et al. Inhibition of EZH2 Promotes Human Embryonic Stem Cell Differentiation into Mesoderm by Reducing H3K27me3. 2018;11(6):1579–80. doi: 10.1016/j.stemcr.2018.11.013. PubMed PMID: 30540964.
31. Rougeot J, Chrispijn N, Aben M, Elurbe D, Andralojc K, Murphy P, et al. Maintenance of spatial gene expression by Polycomb-mediated repression after formation of a vertebrate body plan. 2019;146(19). doi: 10.1242/dev.178590. PubMed PMID: 31488564.
32. Camilleri ET, Dudakovic A, Riester SM, Galeano-Garces C, Paradise CR, Bradley EW, et al. Loss of histone methyltransferase Ezh2 stimulates an osteogenic transcriptional program in chondrocytes but does not affect cartilage development. J Biol Chem. 2018;293(49):19001–11. Epub 2018/10/18. doi:10.1074/jbc.RA118.003909. PubMed PMID: 30327434; PubMed Central PMCID: PMCPMC6295726.
33. Chen L, Wu Y, Wu Y, Wang Y, Sun L, Li FJSr. The inhibition of EZH2 ameliorates osteoarthritis development through the Wnt/β-catenin pathway. 2016;6:29176. doi: 10.1038/srep29176. PubMed PMID: 27539752.

Figures

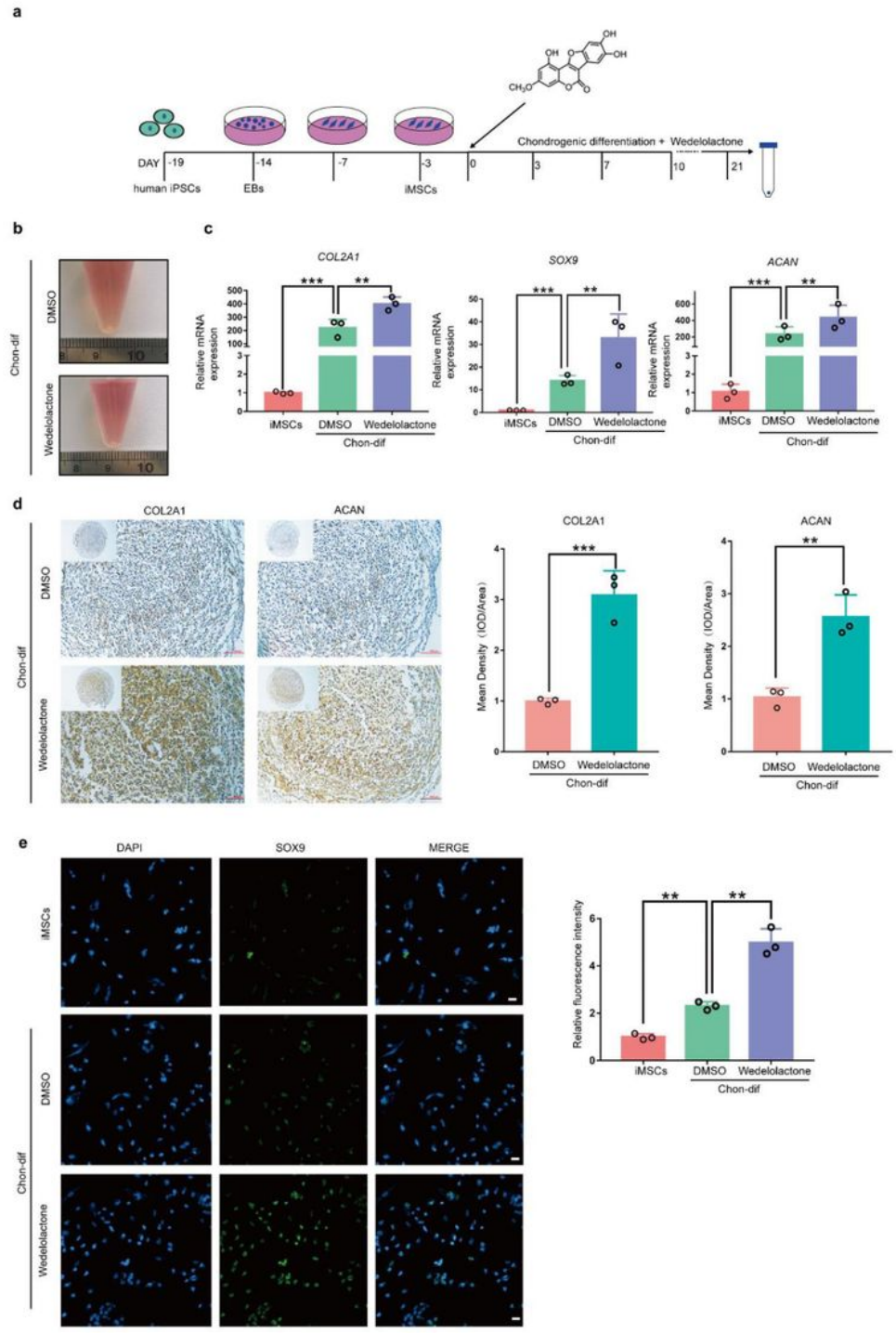

Figure 1

Wedelolactone promotes the differentiation of human induced pluripotent stem cell (iPSC)-derived mesenchymal stem cells (MSCs) to chondrocytes *in vitro*.

(**a**) Schematic procedure of the chondrogenic differentiation of MSCs induced by human iPSC-derived MSCs; EB, embryoid body; iMSCs, human iPSC-derived MSCs; Chon-dif, chondrogenic differentiation.

(**b**) Image of the chondrogenic pellet differentiated from human iPSC-derived MSCs.

(**c**) Gene expression analysis of the chondrogenic differentiation markers (collagen type II alpha-1 (*COL2A1*), SRY-box transcription factor 9 (*SOX9*), and aggrecan (*ACAN*)) in the chondrogenic pellet.

(**d**) Immunohistochemistry image of the chondrogenic pellet stained with COL2A1 and ACAN. Scale bar = 100 μm. Mean density was used to quantify the COL2A1 and ACAN contents in the chondrogenic pellet.

(**e**) Immunofluorescence image of iPSC-derived MSCs under chondrogenic differentiation stained with SOX9, COL2A1, and ACAN. Scale bar = 100 μm. Relative fluorescence intensity was used to quantify the expression levels of SOX9, COL2A1, and ACAN.

Data are expressed as the mean ± standard deviation (SD) (n = 3). Statistical differences were analyzed by one-way analysis of variance (ANOVA) followed by Dunnett's test: *p < 0.05, **p < 0.01, ***p < 0.001.

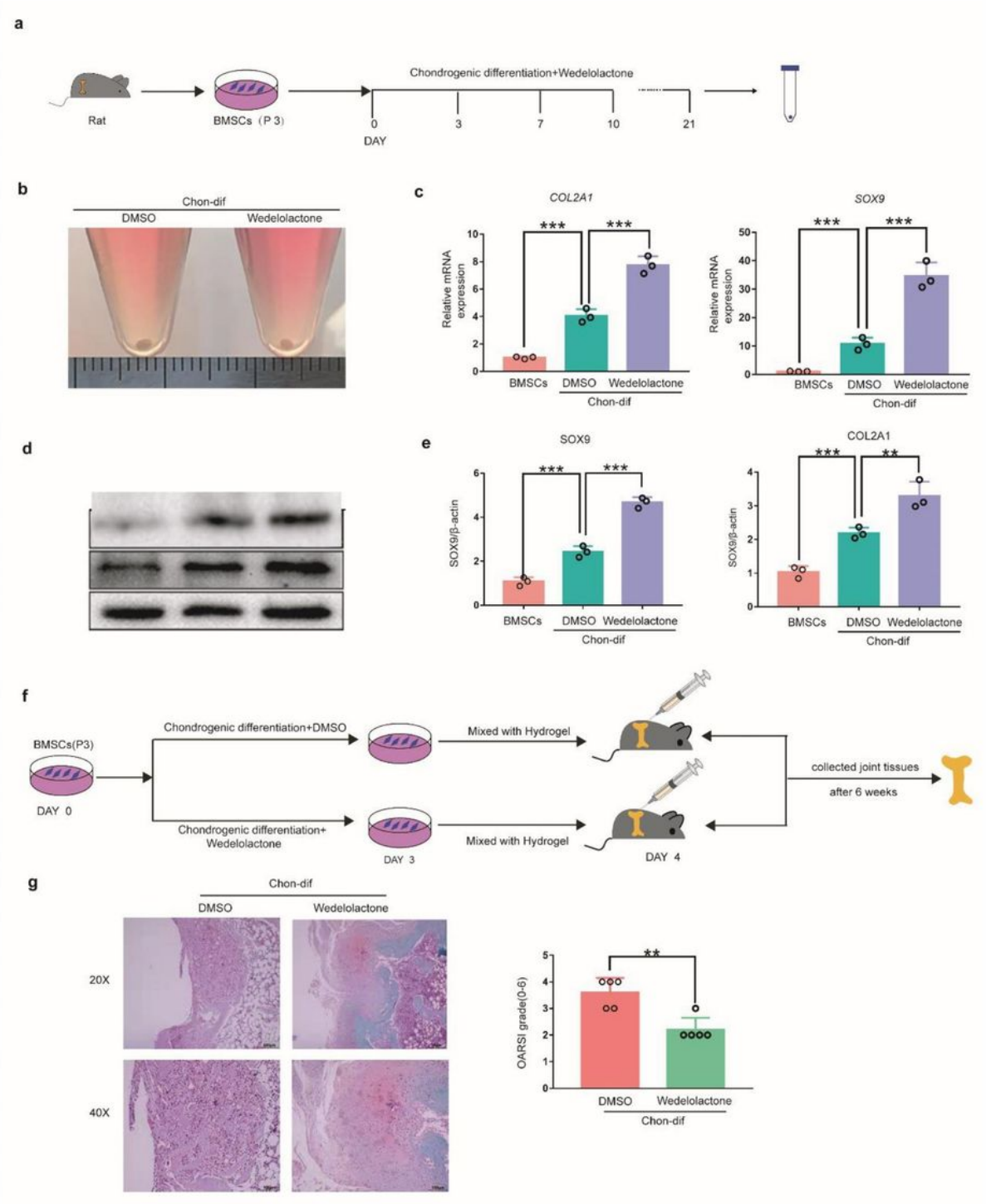

Figure 2

Wedelolactone promotes the chondrogenic differentiation of bone marrow-derived mesenchymal stem cells (BMSCs).

(**a**) Schematic procedure of the chondrogenic differentiation of BMSCs.

(**b**) Image of the chondrogenic pellet differentiated from BMSCs.

(**c**) Gene expression analysis of the chondrogenic differentiation markers (*COL2A1*, *SOX9*, and *ACAN*) in the chondrogenic pellet.

(**d**) Western blotting analysis of the chondrogenic differentiation markers (COL2A1 and SOX9) in the chondrogenic pellet.

(**e**) Mean gray value was used to quantify the protein expression levels of COL2A1 and SOX9 in the chondrogenic pellet.

(**f**) Schematic of the experimental outline. BMSCs treated with dimethyl sulfoxide (DMSO) or wedelolactone were mixed with the hydrogel and transplanted into the cartilage defect model, and the joint tissues were collected after 6 weeks.

(**g**) Safranin-O fast green stains of joints after 6 weeks (n = 5 rat per group). The Osteoarthritis Research Society International scoring system was used to grade the rat cartilage degeneration.

Data are expressed as the mean ± SD (n = 3). Statistical differences were analyzed by one-way ANOVA followed by Dunnett's test: *$p < 0.05$, **$p < 0.01$, ***$p < 0.001$.

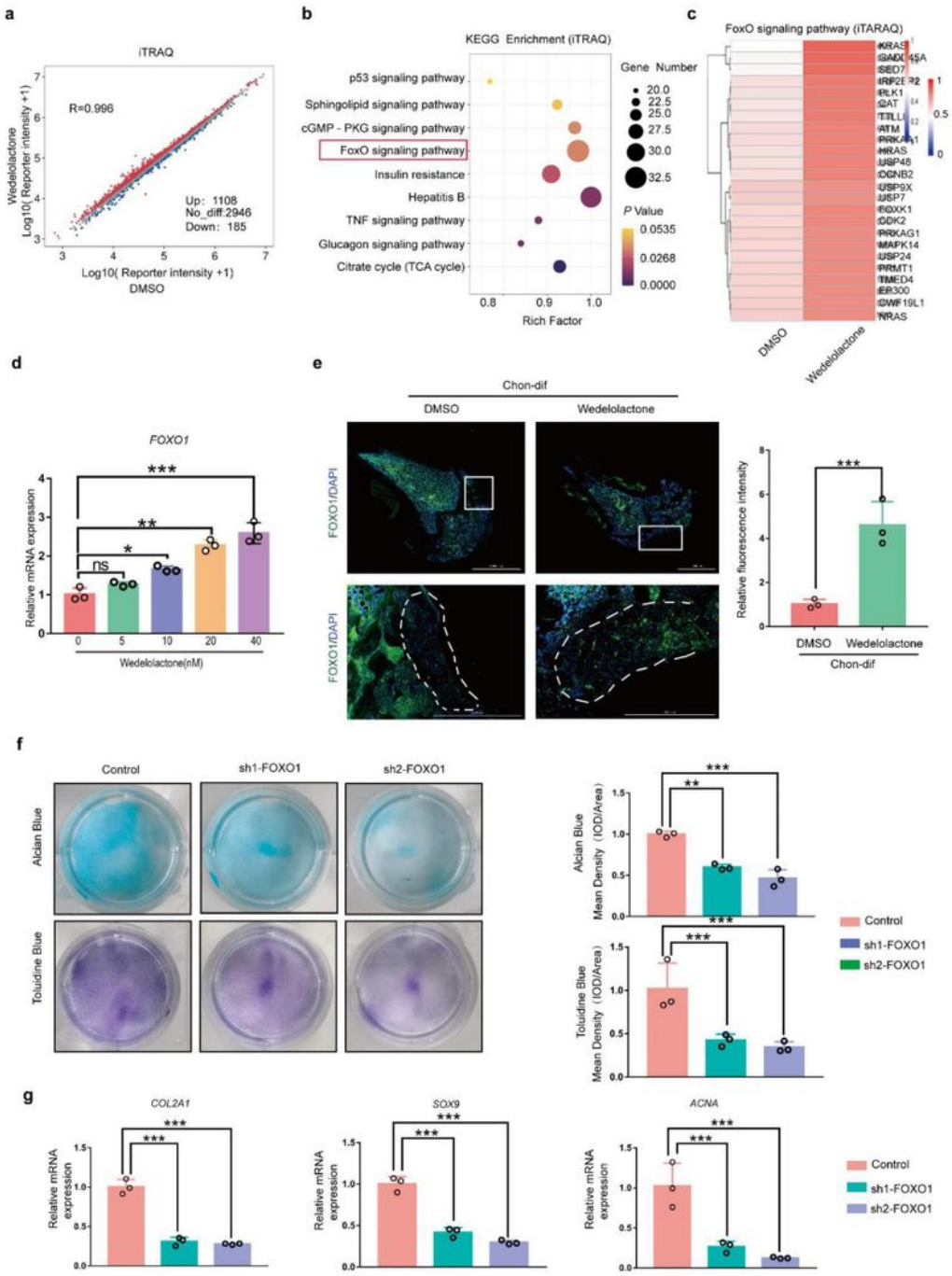

Figure 3

Wedelolactone promotes the chondrogenic differentiation of human iPSC-derived MSCs by activating the forkhead box O (FOXO) pathway.

(**a**) Scatter plot of the quantitation proteomics analysis showing differently expressed proteins in the chondrogenic pellet differentiated from human iPSC-derived MSCs treated with DMSO or wedelolactone.

(**b**) The Kyoto Encyclopedia of Genes and Genomes enrichment analysis of differentially expressed proteins in the chondrogenic pellet differentiated from human iPSC-derived MSCs treated with DMSO or wedelolactone.

(**c**) Heatmap of the quantitation proteomics analysis showing differently expressed proteins associated with FOXO signaling.

(**d**) Gene expression analysis of FOXO1 after induction with different concentrations of wedelolactone.

(**e**) Immunofluorescence staining of FOXO1 in the cartilage defect model after wedelolactone intervention. Scale bar = 100 μm. Relative fluorescence intensity was used to quantify the expression of FOXO1

(**f**) Alcian blue and toluidine blue staining images of the chondrogenic differentiation of human iPSC-derived MSCs after different interventions. Quantification of the mean intensity of alcian blue and toluidine blue staining.

(**g**) Gene expression analysis of the chondrogenic differentiation markers (*COL2A1*, *SOX9*, and *ACAN*) after FOXO1 knockdown. Data are expressed as the mean ± SD (n = 3). Statistical differences were analyzed by one-way ANOVA followed by Dunnett's test: *p < 0.05, **p < 0.01, ***p < 0.001.

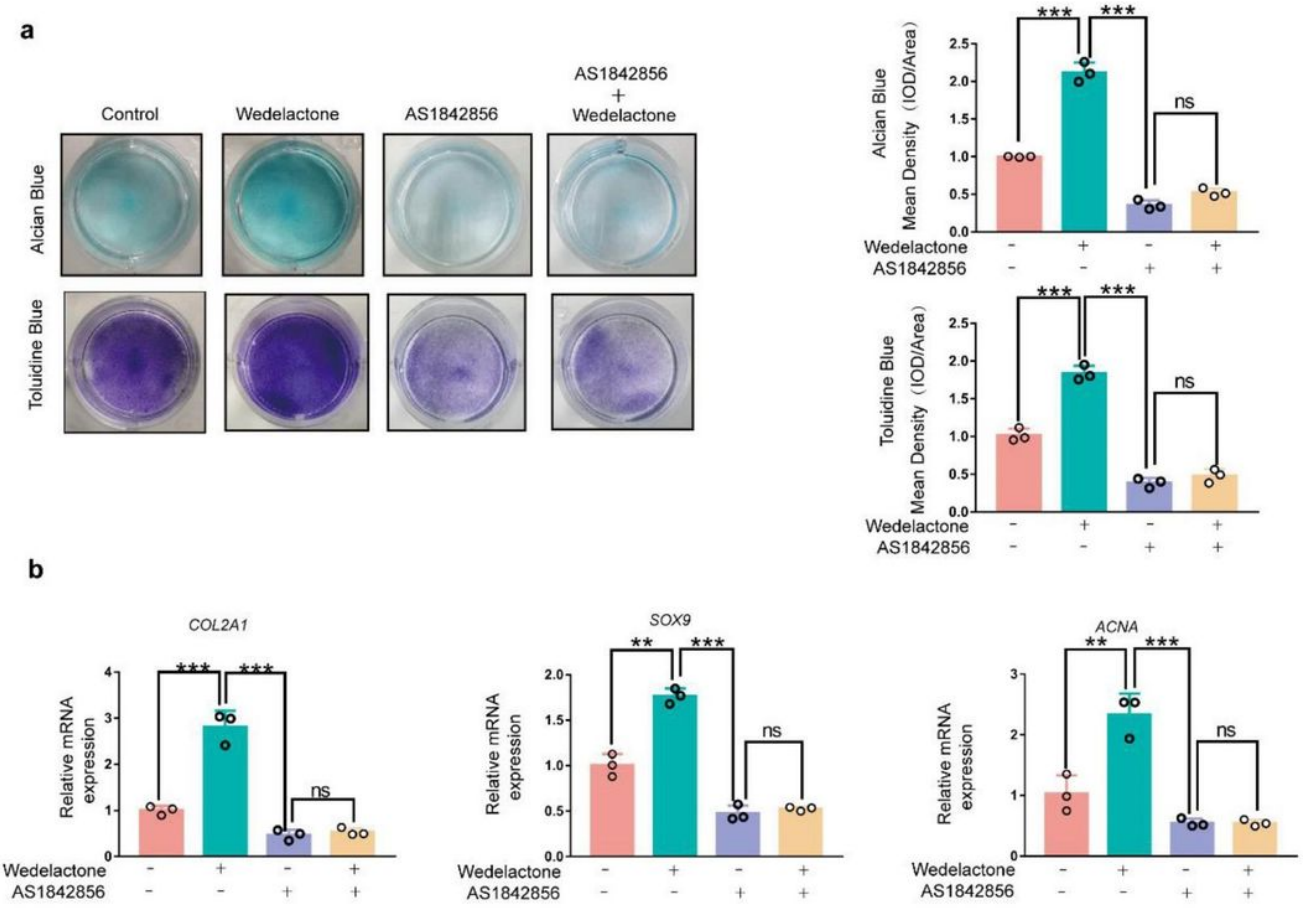

Figure 4

The promoting effect of wedelolactone on chondrogenic differentiation via FOXO1 can be weakened by FOXO1 inhibitors.

(**a**) Alcian blue and toluidine blue staining images of the chondrogenic differentiation of human iPSC-derived MSCs after different interventions. Quantification of the mean intensity of alcian blue and toluidine blue staining.

(**b**) Gene expression analysis of the chondrogenic differentiation markers (*COL2A1*, *SOX9*, and *ACAN*) after wedelolactone and FOXO1 inhibitor (GSK126) intervention. Data are expressed as the mean ± SD (n = 3). Statistical differences were analyzed by one-way ANOVA followed by Dunnett's test: *p < 0.05, **p < 0.01, ***p < 0.001.

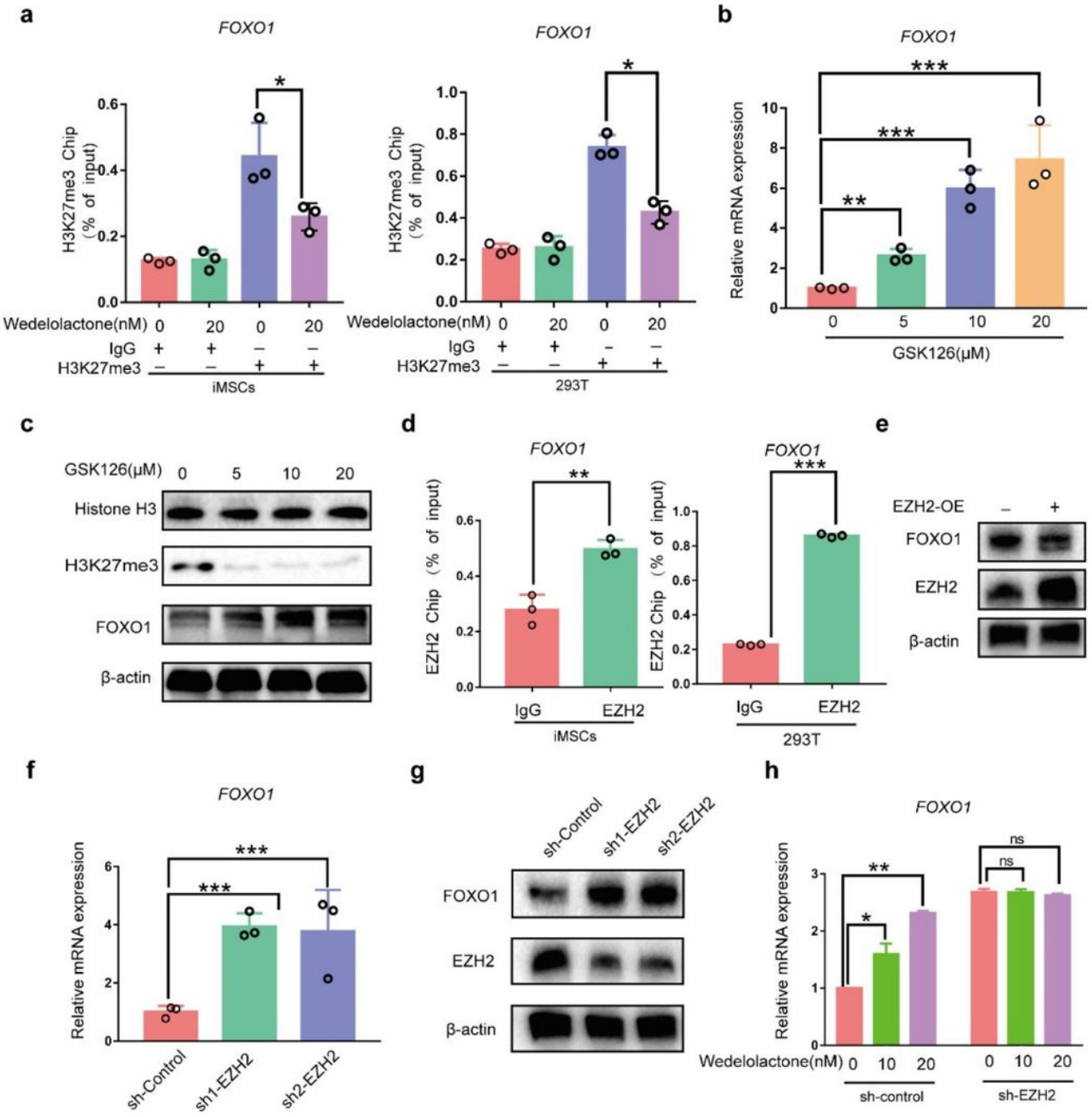

Figure 5

Wedelolactone decreases the enhancer of zeste homolog 2 (EZH2)-dependent trimethylation of histone 3 lysine 27 (H3K27me3) on the promoter region of FOXO1.

(**a**) Chromatin immunoprecipitation-quantitative polymerase chain reaction (ChIP-qPCR) analysis of H3K27me3 enrichment in FOXO1 promoter after wedelolactone intervention in both human iPSC-derived MSCs and 293T cells.

(**b**) Reverse transcription (RT)-qPCR analysis of FOXO1 in human iPSC-derived MSCs after FOXO1 inhibitor (GSK126) intervention.

(**c**) Western blotting analysis of FOXO1 in human iPSC-derived MSCs after FOXO1 inhibitor (GSK126) intervention.

(**d**) ChIP-qPCR analysis of EZH2 occupancy in FOXO1 promoter in both human iPSC-derived MSCs and 293T cells.

(**e**) Western blotting analysis of FOXO1 in human iPSC-derived MSCs after EZH2 overexpression.

(**f**) RT-qPCR analysis of FOXO1 in human iPSC-derived MSCs after EZH2 knockdown.

(**g**) Western blotting analysis of FOXO1 in human iPSC-derived MSCs after EZH2 knockdown.

(**h**) RT-qPCR analysis of FOXO1 in human iPSC-derived MSCs induced with wedelolactone after EZH2 knockdown.

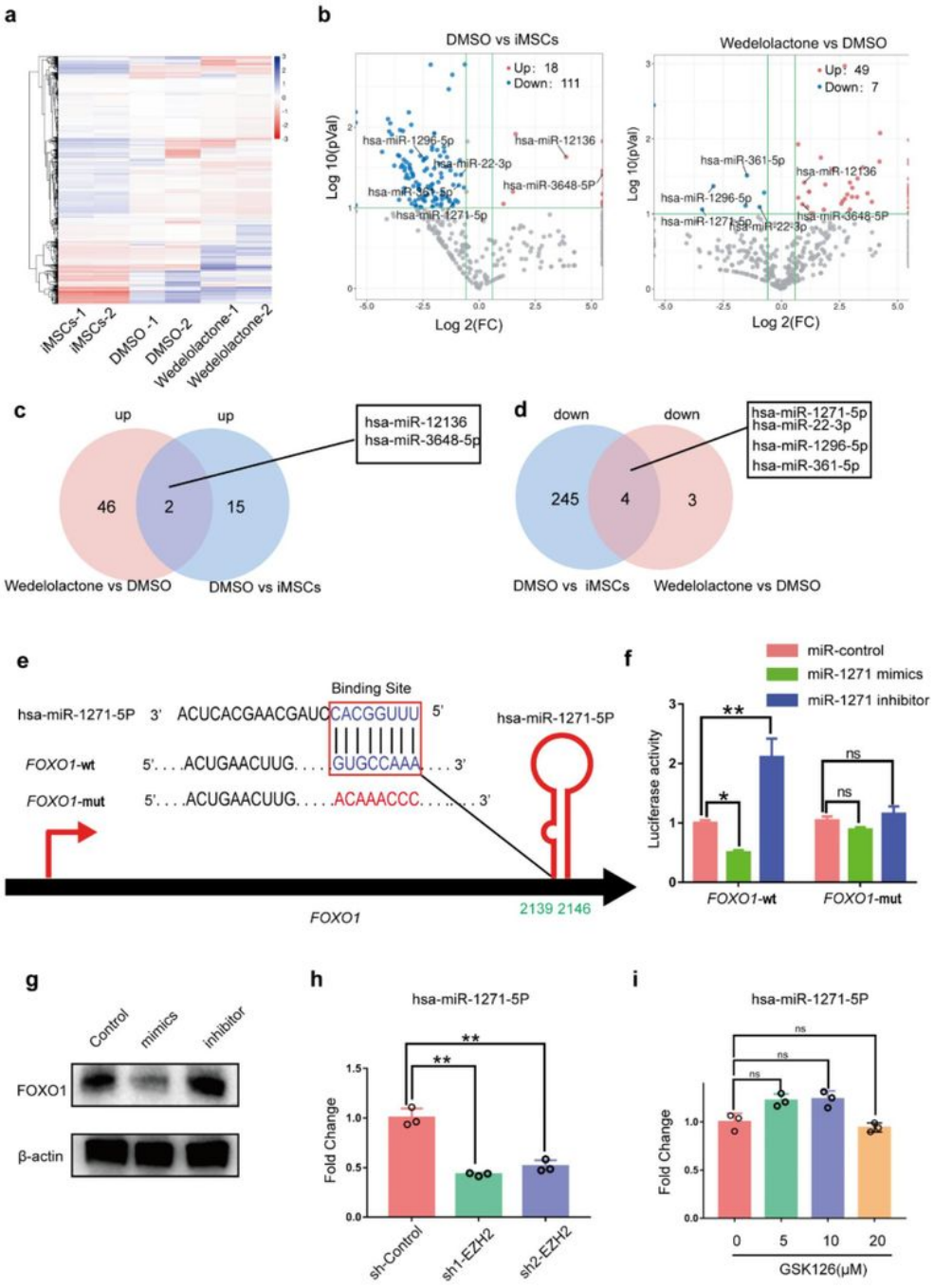

Figure 6

MicroRNA (miR)-1271-5P regulates the expression of FOXO1 via post-transcriptional regulation during chondrogenic differentiation.

(**a**) Heatmap of miRNA-seq analysis, showing the differently expressed miRNAs in the chondrogenic pellet differentiated from human iPSC-derived MSCs, and human iPSC-derived MSCs treated with DMSO

or wedelolactone.

(**b**) Volcano plots showing the differently expressed miRNAs. Red color indicates the significantly upregulated miRNAs, blue color indicates the significantly downregulated miRNAs, and gray color indicates the genes with no differential expression.

(**c**) Venn diagram overlap showing the number of upregulated miRNAs and miRNAs in the DMSO group compared to the human iPSC-derived MSCs and wedelolactone groups.

(**d**) Venn diagram overlap showing the numbers of downregulated miRNAs and miRNAs in the DMSO group compared to the human iPSC-derived MSCs and wedelolactone groups.

(**e**) miR-1271-5P target sequence in the 3'-untranslated region (UTR) of FOXO1 predicted by the TargetScan database.

(**f**) The target of FOXO1 with miR-1271-5P was confirmed by the luciferase reporter assay.

(**g**) Western blotting detection of protein expression levels of FOXO1 in human iPSC-derived MSCs transfected with the miR-1271-5P mimic or inhibitor under chondrogenic differentiation.

(**h**) RT-qPCR analysis of miR-1271-5P in human iPSC-derived MSCs after EZH2 knockdown.

(**i**) RT-qPCR analysis of miR-1271-5P in human iPSC-derived MSCs after FOXO1 inhibitor (GSK126) intervention.

Statistical differences were analyzed by one-way ANOVA followed by Dunnett's test: *p < 0.05, **p < 0.01, ***p < 0.001.

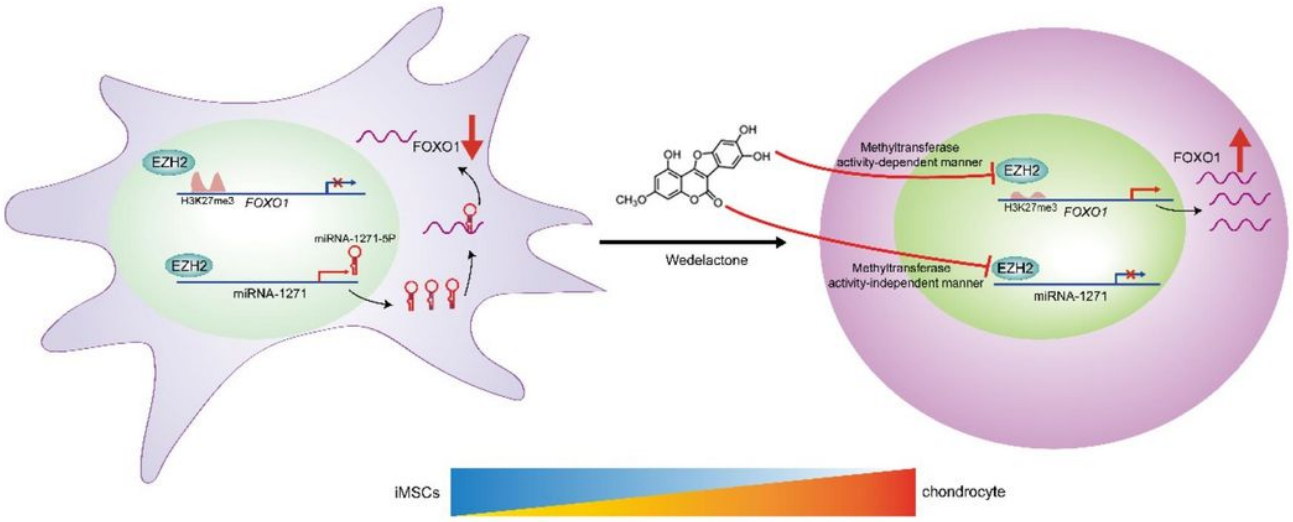

Figure 7

Schematic illustration of the working model.

Supplementary Files

This is a list of supplementary files associated with this preprint. Click to download.

- SupplementaryInformationF.docx